Contribution from the Department of Chemistry,
University of California, Davis, California 95616

X-ray Crystal Structure and Structural Dynamics of $[Ir_3\{\mu\text{-}(Ph_2PCH_2)_2AsPh\}_2(\mu\text{-}CO)_2(CO)_2(\mu\text{-}Cl)Cl]^+$ and Related Rhodium Complexes

Alan L. Balch,* L. Alan Fossett, Rosalvina R. Guimerans, Marilyn M. Olmstead, and Philip E. Reedy, Jr.

Received September 5, 1985

The preparation of the tetracarbonyl complexes $[Ir_3(\mu\text{-dpma})_2(\mu\text{-CO})_2(CO)_2(\mu\text{-X})X][BPh_4]$, $[Rh_3(\mu\text{-dpma})_2(\mu\text{-CO})_2(CO)_2(\mu\text{-I})I][BPh_4]$ and $[Rh_3(\mu\text{-dpmp})_2(\mu\text{-CO})_2(CO)_2(\mu\text{-X})X][BPh_4]$ (dpma = bis((diphenylphosphino)methyl)phenylarsine; dpmp = bis((diphenylphosphino)methyl)phenylphosphine; X = Cl, Br, I) is reported. Infrared and electronic spectral data indicate that all have a common structure. $[Ir_3\{\mu\text{-}((C_6H_5)_2PCH_2)_2AsC_6H_5\}_2(\mu\text{-CO})_2(CO)_2(\mu\text{-Cl})Cl][B(C_6H_5)_4]\cdot 2CH_2Cl_2$ crystallizes from dichloromethane/ether in the triclinic space group $P\bar{1}$ (No. 2) with a = 12.789 (3) Å, b = 16.936 (4) Å, c = 23.874 (6) Å, α = 87.80 (2)°, β = 68.69 (2)°, γ = 77.05 (2)° at 140 K. Least-squares refinement of 493 parameters using 8413 reflections yields R = 0.083, R_w = 0.090. The structure of the cation has the two dpma ligands in a fully extended trans alignment. The three iridium atoms are nearly linear (Ir–Ir–Ir angle 166.0 (1)°) with Ir–Ir bonds of nearly equal lengths, 2.887 (1) and 2.842 (1) Å. One Ir–Ir bond is bridged by a chloride and a carbonyl ligand in a double-A-frame arrangement while the other Ir–Ir bond is bridged by a carbonyl ligand. A nearly statistical disorder in the crystal packing exchanges the sites of the bridging chlorine and the terminal chlorine. Multinuclear (^{31}P, ^1H, and ^{13}C) NMR spectra of these tetracarbonyls in dichloromethane solution indicate that they have a time-averaged, symmetrical structure that renders the two end P_2Ir environments equivalent. A dynamic process involving bridge/terminal halide interchange is proposed to explain these spectra.

Introduction

Through the use of the linear, small-bite ligands bis((diphenylphosphino)methyl)phenylphosphine, dpmp,[1] and bis((diphenylphosphino)methyl)phenylarsine, dpma,[2] it is possible to construct trinuclear chain complexes having $M_3(\mu\text{-dpmp})_2$ or $M_3(\mu\text{-dpma})_2$ cores with the two tridentate ligands in trans alignment bridging the three metals.[2-13] With rhodium, three series of interrelated complexes, $[Rh_3(\mu\text{-dpmp})_2(CO)_nX_2]^+$ (X = Cl, Br, I; n = 2, 3, 4), have been prepared.[3,4,6,9] Each of the dicarbonyls possesses the nonfluxional structure **1**[9] (Chart I). Remarkably, the tricarbonyls have different structures for each of the three different halide ligands. Thus, the chloro tricarbonyl has the chloro-bridged structure **2**,[3,13] while the bromo tricarbonyl has the carbonyl-bridged structure **3**.[13] Both **2** and **3** are fluxional, but in different ways. In solution, **2** undergoes facile bridge/terminal chloride exchange and **3** undergoes selective bridge/terminal carbon monoxide exchange that only involves two of the three carbon monoxide ligands.[13] In contrast, the iodo tricarbonyl possesses the nonfluxional structure **4**.[4]

This article is concerned with the characterization of the tetracarbonyl complexes whose structures were previously unknown. The properties of $[Rh_3(\mu\text{-dpmp})_2(\mu\text{-CO})_2(CO)_2(\mu\text{-X})X]^+$, $[Rh_3(\mu\text{-dpma})_2(\mu\text{-CO})_2(CO)_2(\mu\text{-I})I]^+$, and $[Ir_3(\mu\text{-dpma})_2(\mu\text{-CO})_2(CO)_2(\mu\text{-X})X]^+$ (X = Cl, Br, I) are considered. The iridium complexes were particularly attractive for this study because they were less prone to loss of carbon monoxide.

Results

Synthetic Studies. Addition of $Ir(CO)_2Cl(p\text{-tld})$[14] p-tld = p-toluidine) to a mixture of dpma and sodium tetraphenylborate in dichloromethane/methanol gave orange $[Ir_3(\mu\text{-dpma})_2(\mu\text{-CO})_2(CO)_2(\mu\text{-Cl})Cl][BPh_4]$ in modest yield. Treatment of dichloromethane solutions of this salt with methanol solutions of sodium bromide or sodium iodide produced the corresponding bromide or iodide complexes. The rhodium complexes $[Rh_3(\mu\text{-dpmp})_2(\mu\text{-CO})_2(CO)_2(\mu\text{-X})X]^+$ were prepared by treating dichloromethane solutions of **2**–**4** with carbon monoxide (1 atm). $[Rh_3(\mu\text{-dpma})_2(\mu\text{-CO})_2(CO)_2(\mu\text{-I})I][BPh_4]$ was similarly prepared by the addition of carbon monoxide to the dpma analogue of **4**. For these rhodium compounds the addition of carbon monoxide was reversible; however, the iridium tetracarbonyl complexes showed no evidence for carbon monoxide loss under comparable conditions. Warming of dichloromethane solutions of $[Rh_3(\mu\text{-dpmp})_2(\mu\text{-CO})_2(CO)_2(\mu\text{-X})X]^+$ causes the loss of carbon monoxide and the re-formation of **2**–**4**. The reversibility is demonstrated in Figure 1, which shows the electronic spectrum of **3** in dichloromethane solution in trace A. Trace B shows the spectrum of $[Rh_3(\mu\text{-dpmp})_2(\mu\text{-CO})_2(CO)_2(\mu\text{-Br})Br]^+$ formed by the addition of carbon monoxide, while trace C shows the same sample after gentle warming for a few minutes. The similarity of traces A and C establishes the reversibility of the reaction. The stability of these rhodium tetracarbonyls toward carbon monoxide loss decreases in the order $I^- > Br^- > Cl^-$. Because $[Rh_3(\mu\text{-dpmp})_2(\mu\text{-CO})_2(CO)_2(\mu\text{-Cl})Cl]^+$ loses carbon monoxide so readily, it was not possible to isolate this species in pure solid form. Electronic spectral data for the tetracarbonyl complexes are collected in Table I.

Table I also contains the infrared spectral data for the carbonyl stretching region of these complexes. All complexes show similar features. Two bands due to bridging carbon monoxide are observed at ca. 1815 and 1730 cm^{-1} for the iridium complexes and at ca. 1850 and 1780 cm^{-1} for the rhodium complexes. A set of bands due to terminal carbon monoxide ligands at ca. 1970 cm^{-1} are also present.

The electronic and infrared spectra of these complexes as mineral oil mulls and in dichloromethane solutions are similar. Consequently, the same structural features are present in both the solids and in solutions. The observation of additional peaks in the solid-state infrared spectra probably arises from different local site symmetries and is consistent with the observed disorder

(1) Appel, R.; Geisler, K.; Scholer, H.-F. *Chem. Ber.* **1979**, *112*, 648.
(2) Balch, A. L.; Fossett, L. A.; Olmstead, M. M.; Oram, D. E.; Reedy, P. E. *J. Am. Chem. Soc.* **1985**, *107*, 5272.
(3) Guimerans, R. R.; Olmstead, M. M.; Balch, A. L. *J. Am. Chem. Soc.* **1983**, *105*, 1677.
(4) Olmstead, M. M.; Guimerans, R. R.; Balch, A. L. *Inorg. Chem.* **1983**, *22*, 2473.
(5) Olmstead, M. M.; Guimerans, R. R.; Farr, J. P.; Balch, A. L. *Inorg. Chim. Acta* **1983**, *75*, 199.
(6) Balch, A. L.; Guimerans, R. R.; Olmstead, M. M. *J. Organometal. Chem.* **1984**, *268*, C38.
(7) Balch, A. L.; Olmstead, M. M.; Guimerans, R. R. *Inorg. Chim. Acta* **1984**, *84*, L21.
(8) Balch, A. L.; Guimerans, R. R.; Linehan, J. *Inorg. Chem.* **1985**, *24*, 290.
(9) Balch, A. L.; Fossett, L. A.; Guimerans, R. R.; Olmstead, M. M. *Organometallics* **1985**, *4*, 781.
(10) Balch, A. L.; Olmstead, M. M. *Isr. J. Chem.* **1985**, *25*, 189.
(11) Balch, A. L.; Linehan, J.; Olmstead, M. M. *Inorg. Chem.* **1985**, *24*, 3975.
(12) Balch, A. L.; Fossett, L. A.; Linehan, J.; Olmstead, M. M. *Organometallics*, in press.
(13) Balch, A. L.; Fossett, L. A.; Guimerans, R. R.; Olmstead, M. M.; Reedy, P. E., Jr.; Wood, F. E. *Inorg. Chem.*, in press.
(14) Klabunde, U. *Inorg. Synth.* **1974**, *15*, 82.

0020-1669/86/1325-1397$01.50/0

Chart I

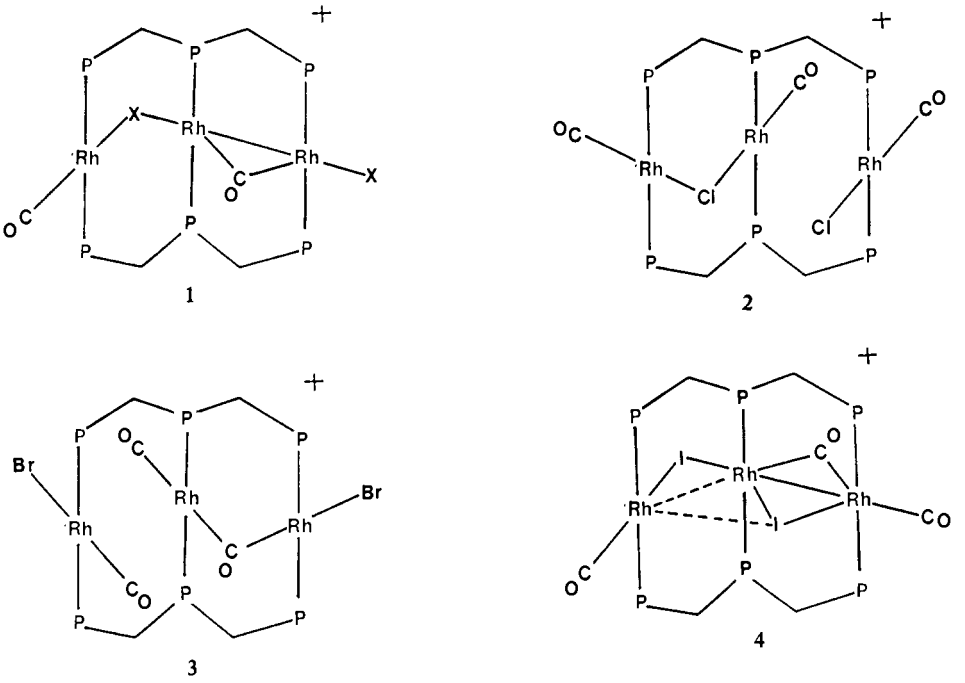

Table I. Infrared and Electronic Spectral Data for Tetracarbonyl Complexes

compd	Ir ν(CO), cm^{-1} terminal	Ir ν(CO), cm^{-1} bridging	UV–vis[b] λ_{max}, nm (ϵ, M^{-1} cm^{-1})
$[Rh_3(\mu\text{-dpmp})_2(\mu\text{-CO})_2(CO)_2(\mu\text{-Cl})Cl][BPh_4]$	1988[b]	1864, 1793[b]	528 (18 000), 389 (14 500)
$[Rh_3(\mu\text{-dpmp})_2(\mu\text{-CO})_2(CO)_2(\mu\text{-Br})Br][BPh_4]$	1981 sh, 1968[a] 1984[b]	1847, 1832, 1763[a] 1849, 1783[b]	526 (16 800), 392 (39 200)
$[Rh_3(\mu\text{-dpmp})_2(\mu\text{-CO})_2(CO)_2(\mu\text{-I})I][BPh_4]$	1980[a] 1987[b]	1845 sh, 1825, 1778[a] 1860 sh, 1838, 1775[b]	512 (13 300), 382 (21 700)
$[Rh_3(\mu\text{-dmpa})_2(\mu\text{-CO})_2(CO)_2(\mu\text{-I})I][BPh_4]$	1991, 1978[a]	1828, 1775[a]	550 (6800), 440 (10 300), 397 (18 700), 307 (24 100) 605, 570, 445, 410[a]
$[Ir_3(\mu\text{-dpma})_2(\mu\text{-CO})_2(CO)_2(\mu\text{-Cl})Cl][BPh_4]$	1968, 1961[a] 1974[b]	1822, 1799, 1736, 1727, 1717[a] 1814, 1736[b]	430 (14 600), 369 (16 000) 450, 378[a]
$[Ir_3(\mu\text{-dpma})_2(\mu\text{-CO})_2(CO)_2(\mu\text{-Br})Br][BPh_4]$	1988, 1982, 1978, 1970, 1952[a]	1807, 1790, 1736, 1723[a]	428 (15 400), 366 (20 600) 445, 380[a]
$[Ir_3(\mu\text{-dpma})_2(\mu\text{-CO})_2(CO)_2(\mu\text{-I})I][BPh_4]$	1976, 1963[a]	1811, 1785, 1732[a]	442 (13 500), 370 (24 600) 470, 376[a]

[a] From mineral oil mulls. [b] From dichloromethane solutions.

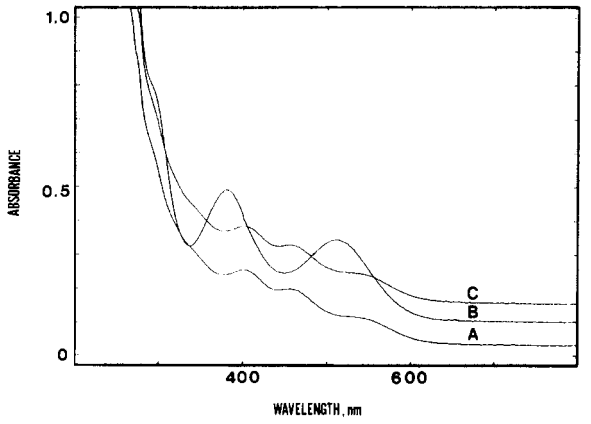

Figure 1. Electronic absorption spectra of 2.2×10^{-4} M solutions of $[Rh_3(\mu\text{-dpmp})_2(\mu\text{-CO})(CO)_2Br_2][BPh_4]$ in dichloromethane: (A) by itself; (B) after exposure to 1 atm of carbon monoxide; (C) after warming to 38 °C. The cell pathlength was 1.0 mm. Traces B and C are offset.

in the solid-state structure of $[Ir_3(\mu\text{-dpma})_2(\mu\text{-CO})_2(CO)_2(\mu\text{-Cl})Cl][BPh_4]$ (vide infra).

X-ray Crystal Structure of $[Ir_3(\mu\text{-dpma})_2(\mu\text{-CO})_2(CO)_2(\mu\text{-Cl})Cl][BPh_4]\cdot 2CH_2Cl_2$. The solid contains one cation, one tetraphenylborate anion (with normal characteristics deserving of no further attention), and four sites that are partially occupied by dichloromethane molecules. There are no unusual contacts be-

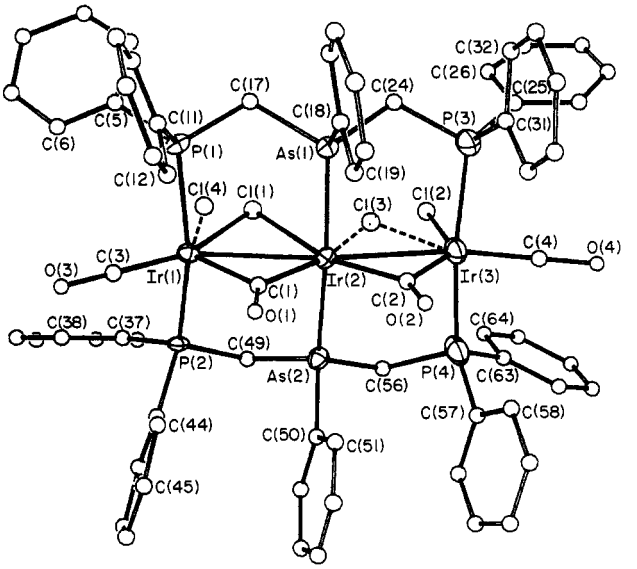

Figure 2. Perspective view of $[Ir_3(\mu\text{-dpma})_2(\mu\text{-CO})_2(CO)_2(\mu\text{-Cl})Cl]^+$ showing the atomic labeling scheme.

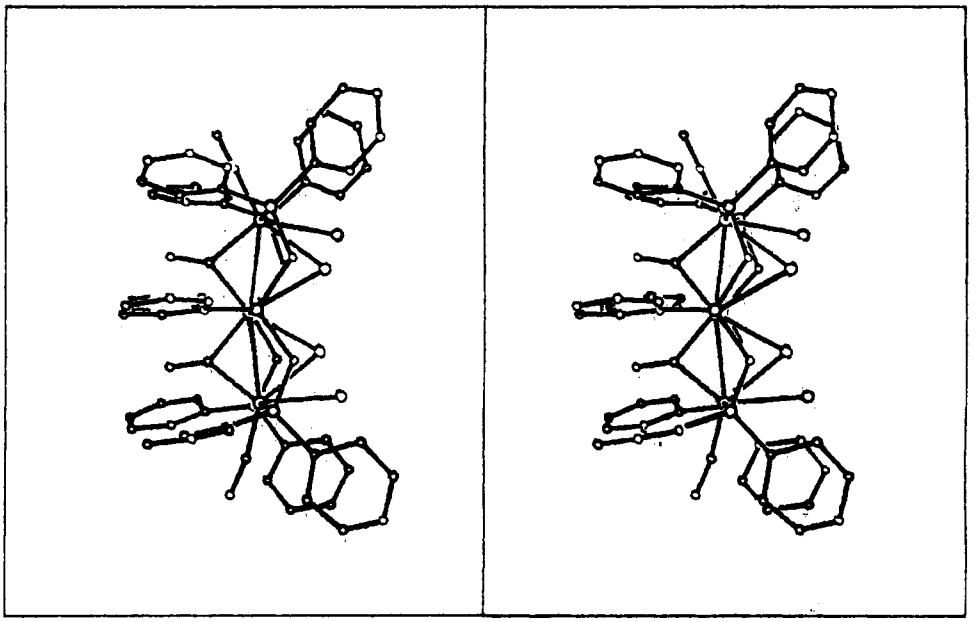

Figure 3. Stereoscopic drawing of $[Ir_3(\mu\text{-dpma})_2(\mu\text{-}CO)_2(CO)_2(\mu\text{-}Cl)Cl]^+$.

tween these units. A drawing that shows the atom-numbering scheme for the cation is shown in Figure 2. Atomic positional parameters appear in Table II. Tables III and IV present selected interatomic distances and angles.

The chloride ligands in the complex cation are disordered. There are two sets of alternative sites. The major site, which has 54.8 (7)% occupancy, involves Cl(1) and Cl(2) and is connected to other atoms by solid lines in all drawings. The minor site, with a 45.2 (7)% occupancy, involves Cl(3) and Cl(4) and is connected to other bonded atoms by dashed lines in the drawings. The individual cations have no crystallographically imposed symmetry. However, there is a virtual mirror plane running through the $Ir_3(CO)_4Cl_2$ core. This is particularly evident in the stereoscopic drawing shown in Figure 3. The orientation of its perspective is such that the cation is viewed nearly perpendicularly to the virtual mirror plane.

As we have noted for other trinuclear complexes,[2,9] the overall geometry of the cation can be related to the structure of related phosphine-bridged binuclear complexes. The left side (as shown in Figure 2), including Ir(1), all of its ligands, Ir(2), As(1), and As(2), resembles the double A-frames $Ir_2(\mu\text{-dpm})_2(\mu\text{-}CO)(\mu\text{-}S)(CO)_2$ (**5a**)[15] and $Rh_2(\mu\text{-dpm})_2(\mu\text{-}CO)(\mu\text{-}Cl)(CO)_2^+$ (**5b**)[16]

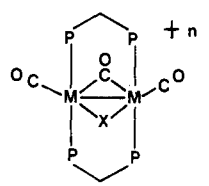

5a: M = Ir, X = S, n = 0
5b: M = Rh, X = Cl, n = 1

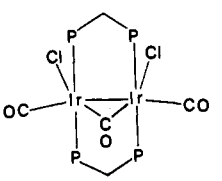

6

(dpm is bis(diphenylphosphino)methane). The similarity includes not only the $Ir_2(\mu\text{-}CO)(\mu\text{-}X)$ core but extends to the orientation of the terminal carbonyl groups (on the same side of the Ir–Ir vector as the bridging carbonyl), the orientation of the phenyl rings, and the location of the methylene bridges (over the Cl or S bridges rather than over the carbonyl bridge). The right side of the cation, including Ir(3) and its ligands as well as Ir(2), As(1), and As(2), resembles the carbonyl-bridged A-frame $Ir_2(\mu\text{-dpm})_2(\mu\text{-}CO)(CO)_2Cl_2$[17] (**6**) and to a lesser extent $Rh_2(\mu\text{-dpm})_2(\mu\text{-}CO)X_2$ (X = Cl,[18] Br[19]).

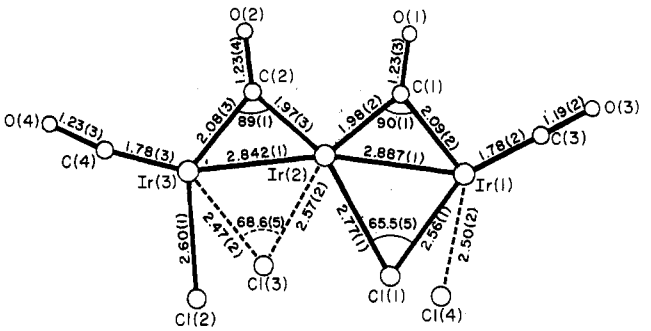

Figure 4. Drawing of the nearly planar $Ir_3(CO)_4Cl_2$ section of $[Ir_3(\mu\text{-dpma})_2(\mu\text{-}CO)_2(CO)_2(\mu\text{-}Cl)Cl]^+$.

Some aspects of the geometry within the planar $Ir_3(CO)_4Cl_2$ unit are shown in Figure 4. Each of the three iridium atoms resides in a unique environment. The Ir_3 chain is nearly linear with an Ir(1)–Ir(2)–Ir(3) angle of 166.0 (1)°. The two Ir–Ir separations, 2.887 (1) and 2.842 (1) Å, are nearly equal, and their lengths are consistent with the presence of Ir–Ir single bonds. Comparable distances in the 2.72–2.85-Å range are found in other iridium or rhodium compounds containing carbonyl bridges.[15-19] Unlike the case in the dimers **5** and **6**, where the carbonyl bridges are nearly symmetrically placed between the two metals, both of the bridging carbonyls in $[Ir_3(\mu\text{-dpma})_2(\mu\text{-}CO)_2(CO)_2(\mu\text{-}Cl)Cl]^+$ are asymmetrically situated. The bridging chloride is also asymmetrically placed, but in the opposite way. While Ir–Cl–Ir angles are quite acute, they are comparable to that in **5b**, 67.4 (1)°.[16]

The $Ir_3(\mu\text{-dpma})_2$ unit has the two tridentate ligands aligned so that the Ir–P and Ir–As vectors are nearly normal to the $Ir_3(CO)_4Cl_2$ plane. The As(1)–Ir(2)–As(2) angle (173.8 (1)°) is nearly linear, but the P–Ir–P angles (162.2 (2), 169.6 (2)°) show somewhat more bending. That bending is due to the fact that the end iridium atoms are bonded to and pulled toward the central iridium. Thus the Ir(1)–Ir(2) and Ir(2)–Ir(3) distances are both significantly shorter than the corresponding nonbonded P···As distances. These distances are comparable to the nonbonded P···As distances (3.073 (6), 3.068 (6) Å and 3.093 (9), 3.087 (9) Å) in $PtRh(\mu\text{-}Ph_2PCH_2AsPh_2)_2(CO)X_3$ (X = Cl, I), where the ligand bridges Rh–Pt bonds 2.692 (1) and 2.737 (3) Å long,[20] but they

(15) Kubiak, C. P.; Woodcock, C.; Eisenberg, R. *Inorg. Chem.* **1980**, *19*, 2733.
(16) Olmstead, M. M.; Lindsay, C. H.; Benner, L. S.; Balch, A. L. *J. Organomet. Chem.* **1979**, *179*, 289.
(17) Sutherland, B. R.; Cowie, M. *Inorg. Chem.* **1984**, *23*, 234.
(18) Gelmini, L.; Stephan, D. W.; Loeb, S. J. *Inorg. Chim. Acta* **1985**, *98*, L3.
(19) Cowie, M.; Dwight, S. K. *Inorg. Chem.* **1980**, *19*, 2508.

Table II. Atomic Coordinates ($\times 10^4$) and Isotropic Thermal Parameters ($Å^2 \times 10^3$) for $[Ir_3\{\mu\text{-}(Ph_2PCH_2)_2AsPh\}_2(\mu\text{-}CO)_2(CO)_2(\mu\text{-}Cl)Cl][BPh_4]\cdot 4CH_2Cl_2$

atom	x	y	z	U^a	atom	x	y	z	U^a
Ir(1)	7014 (1)	30 (1)	1479 (1)	19 (1)*	C(36)	1185 (27)	1980 (21)	3635 (13)	57 (9)
Ir(2)	4807 (1)	66 (1)	2419 (1)	17 (1)*	C(37)	8833 (20)	−1878 (14)	978 (10)	20 (5)
Ir(3)	2972 (1)	−90 (1)	3502 (1)	31 (1)*	C(38)	9653 (22)	−1689 (17)	459 (11)	36 (7)
As(1)	4867 (2)	1356 (2)	2778 (1)	24 (1)*	C(39)	10824 (23)	−2130 (16)	248 (11)	34 (7)
As(2)	4937 (2)	−1293 (2)	2076 (1)	23 (1)*	C(40)	11115 (24)	−2782 (17)	569 (11)	39 (7)
P(1)	7260 (6)	1256 (4)	1785 (3)	23 (3)*	C(41)	10304 (22)	−2990 (16)	1111 (11)	35 (7)
P(2)	7350 (5)	−1321 (4)	1169 (3)	18 (2)*	C(42)	9161 (22)	−2526 (15)	1286 (11)	30 (6)
P(3)	2964 (7)	1107 (5)	3966 (3)	37 (3)*	C(43)	7051 (19)	−1511 (13)	501 (9)	16 (5)
P(4)	2852 (7)	−1375 (5)	3213 (3)	40 (3)*	C(44)	6443 (20)	−914 (15)	266 (10)	26 (6)
Cl(1)	6940 (11)	−462 (8)	2518 (5)	40	C(45)	6155 (21)	−1071 (15)	−223 (10)	26 (6)
Cl(2)	4373 (11)	−832 (8)	4014 (5)	40	C(46)	6499 (22)	−1806 (16)	−506 (11)	33 (6)
Cl(3)	5017 (13)	−604 (10)	3370 (7)	40	C(47)	7170 (21)	−2449 (15)	−288 (10)	27 (6)
Cl(4)	7885 (13)	−573 (10)	2224 (7)	40	C(48)	7457 (21)	−2305 (15)	217 (10)	26 (6)
Cl(5)	8547 (12)	1076 (9)	3702 (6)	70	C(49)	6542 (21)	−1885 (15)	1761 (11)	30 (6)
Cl(6)	6216 (12)	1586 (9)	4575 (6)	70	C(50)	4310 (20)	−1465 (15)	1487 (10)	24 (6)
Cl(7)	3016 (12)	5475 (9)	10974 (6)	70	C(51)	3535 (21)	−833 (16)	1350 (10)	29 (6)
Cl(8)	3445 (12)	4411 (9)	9934 (6)	70	C(52)	3084 (21)	−927 (15)	908 (10)	24 (6)
Cl(9)	998 (19)	4436 (14)	5497 (9)	70	C(53)	3339 (22)	−1682 (16)	663 (11)	33 (6)
Cl(10)	−1144 (19)	4375 (14)	6490 (9)	70	C(54)	4098 (23)	−2343 (18)	800 (11)	40 (7)
Cl(11)	3792 (22)	3105 (15)	5105 (11)	70	C(55)	4565 (19)	−2199 (14)	1204 (9)	20 (5)
Cl(12)	3614 (22)	4456 (15)	4269 (11)	70	C(56)	4300 (23)	−1978 (17)	2742 (11)	40 (7)
O(1)	4812 (12)	717 (9)	1229 (6)	19 (4)	C(57)	1936 (23)	−1371 (17)	2788 (11)	38 (7)
O(2)	2404 (16)	720 (11)	2453 (8)	43 (5)	C(58)	1065 (23)	−681 (18)	2796 (12)	41 (7)
O(3)	8231 (15)	378 (11)	205 (7)	33 (4)	C(59)	347 (25)	−673 (18)	2469 (12)	45 (8)
O(4)	495 (18)	126 (12)	4312 (9)	53 (6)	C(60)	538 (28)	−1391 (20)	2134 (14)	60 (9)
C(1)	5283 (19)	404 (13)	1574 (9)	16 (5)	C(61)	1393 (28)	−2002 (21)	2122 (14)	63 (9)
C(2)	3117 (23)	370 (17)	2664 (11)	38 (7)	C(62)	2113 (28)	−2047 (20)	2430 (13)	56 (9)
C(3)	7748 (19)	232 (13)	716 (9)	16 (5)	C(63)	2443 (21)	−2073 (14)	3817 (9)	70
C(4)	1540 (24)	−29 (17)	4016 (12)	41 (7)	C(64)	3237 (21)	−2449 (14)	4074 (9)	70
C(5)	8773 (21)	1218 (15)	1694 (10)	29 (6)	C(65)	2915 (21)	−2953 (14)	4553 (9)	70
C(6)	9601 (19)	986 (13)	1175 (9)	17 (5)	C(66)	1798 (21)	−3081 (14)	4775 (9)	70
C(7)	10726 (24)	1012 (16)	1109 (12)	38 (7)	C(67)	1005 (21)	−2705 (14)	4518 (9)	70
C(8)	11002 (24)	1281 (16)	1552 (11)	34 (7)	C(68)	1327 (21)	−2201 (14)	4039 (9)	70
C(9)	10087 (25)	1524 (18)	2094 (13)	49 (8)	C(69)	2753 (25)	5389 (18)	6977 (12)	44 (7)
C(10)	8977 (22)	1528 (15)	2184 (11)	29 (6)	C(70)	3164 (27)	6043 (20)	7001 (14)	58 (9)
C(11)	6851 (20)	2188 (15)	1411 (10)	24 (6)	C(71)	3288 (26)	6636 (19)	6554 (12)	51 (8)
C(12)	6144 (21)	2188 (16)	1082 (10)	30 (6)	C(72)	2901 (24)	6572 (18)	6093 (12)	43 (7)
C(13)	5813 (23)	2913 (16)	825 (11)	36 (7)	C(73)	2432 (25)	5958 (18)	6065 (13)	49 (8)
C(14)	6233 (25)	3580 (19)	881 (12)	46 (8)	C(74)	2364 (26)	5339 (19)	6534 (12)	51 (8)
C(15)	6929 (25)	3565 (18)	1187 (12)	46 (8)	C(75)	3772 (26)	4488 (18)	7626 (13)	48 (8)
C(16)	7251 (24)	2846 (16)	1438 (11)	39 (7)	C(76)	4761 (31)	4315 (22)	7165 (17)	79 (11)
C(17)	6453 (19)	1471 (14)	2570 (9)	20 (5)	C(77)	5934 (35)	4134 (24)	7117 (18)	83 (12)
C(18)	4064 (22)	2372 (16)	2572 (11)	33 (6)	C(78)	6005 (35)	4072 (23)	7673 (15)	78 (11)
C(19)	3374 (21)	2376 (15)	2245 (10)	28 (6)	C(79)	5126 (32)	4208 (23)	8176 (18)	83 (12)
C(20)	2812 (27)	3123 (19)	2110 (13)	53 (8)	C(80)	3974 (28)	4406 (19)	8141 (14)	58 (9)
C(21)	3010 (27)	3801 (20)	2239 (13)	57 (9)	C(81)	2175 (23)	3987 (17)	7357 (11)	37 (7)
C(22)	3780 (27)	3791 (21)	2530 (14)	62 (9)	C(82)	2916 (25)	3233 (17)	7103 (11)	40 (7)
C(23)	4271 (26)	3089 (18)	2706 (13)	49 (8)	C(83)	2252 (24)	2588 (18)	6946 (11)	41 (7)
C(24)	4321 (23)	1385 (18)	3646 (11)	41 (7)	C(84)	1470 (28)	2649 (21)	7030 (14)	62 (9)
C(25)	2689 (26)	1024 (18)	4745 (12)	46 (8)	C(85)	634 (27)	3347 (18)	7288 (12)	48 (8)
C(26)	3588 (32)	821 (21)	4982 (15)	67 (10)	C(86)	999 (23)	4014 (17)	7464 (11)	36 (7)
C(27)	3336 (33)	726 (22)	5594 (15)	72 (10)	C(87)	1536 (21)	5184 (15)	8162 (10)	26 (6)
C(28)	2296 (28)	840 (20)	5985 (15)	59 (9)	C(88)	1180 (24)	4699 (19)	8667 (12)	45 (8)
C(29)	1507 (29)	998 (19)	5790 (14)	55 (9)	C(89)	388 (26)	5026 (19)	9199 (14)	54 (8)
C(30)	1621 (30)	1094 (20)	5195 (14)	61 (9)	C(90)	−124 (30)	5851 (21)	9265 (15)	65 (10)
C(31)	1937 (24)	2020 (17)	3916 (12)	40 (7)	C(91)	138 (24)	6338 (18)	8784 (12)	42 (7)
C(32)	1954 (26)	2776 (18)	4145 (13)	49 (8)	C(92)	988 (23)	6022 (17)	8199 (12)	40 (7)
C(33)	1260 (28)	3455 (22)	4053 (14)	64 (10)	C(93)	7707	1152	4454	70
C(34)	558 (33)	3433 (26)	3752 (16)	83 (12)	C(94)	2445	4975	10505	70
C(35)	474 (29)	2727 (21)	3551 (14)	63 (10)	B	2574 (27)	4746 (19)	7532 (13)	32 (7)

[a] Asterisks designate equivalent isotropic U values, defined as one-third of the trace of the orthogonalized U_{ij} tensors.

are shorter than the P···As distances, 3.254 (4) and 3.283 (4) Å, in the isomeric $Rh(CO)Cl(\mu\text{-}Ph_2AsCH_2PPh_2)_2PtCl_2$, in which no Rh–Pt bond is present and the Rh···Pt separation is longer, 3.043 (1) Å.[21]

The two dpma ligands are aligned trans to one another in a fully extended PCAsCP chain. The $Ir_3(\mu\text{-dpma})_2$ unit takes on the idealized C_{2v} type structure (see structural diagram **5** of ref 9) that is present in other trinuclear complexes, including $[Rh_3(\mu\text{-dpmp})_2(CO)_3(\mu\text{-Cl})Cl]^+$[3] and $[Rh_3(\mu\text{-dpmp})_2(\mu\text{-CO})_2(CO)(\mu\text{-}S_2COEt)(S_2COEt)]^+$,[5] in which the M–M–M angles are greater than 155°.

Multinuclear NMR Studies. The NMR data from ^{31}P and ^1H studies are collected in Table V. The ^{31}P NMR spectrum of $[Ir_3(\mu\text{-dpma})_2(\mu\text{-CO})_2(CO)_2(\mu\text{-Cl})Cl]^+$ consists of a single resonance both at +25 and at −75 °C. Similarly, the spectra of the bromo and iodo analogues show only sharp, single-line resonances at both +25 and −75 °C. The ^{13}C NMR spectrum of ^{13}CO-enriched $[Ir_3(\mu\text{-dpma})_2(\mu\text{-CO})_2(CO)_2(\mu\text{-Cl})Cl]^+$ consists of a triplet at 173.6 ppm due to the terminal carbonyls and an equally intense

(20) Balch, A. L.; Guimerans, R. R.; Linehan, J.; Olmstead, M. M.; Oram, D. E. *Organometallics* **1985**, *4*, 1445.
(21) Balch, A. L.; Guimerans, R. R.; Linehan, J.; Wood, F. E. *Inorg. Chem.* **1985**, *24*, 2021.

Table III. Selected Interatomic Distances (Å) for $[Ir_3(\mu\text{-dpma})_2(\mu\text{-CO})_2(CO)_2(\mu\text{-Cl})Cl]^+$

		At Ir(1)	
Ir(1)–Ir(2)	2.887 (1)	Ir(1)–P(1)	2.350 (7)
Ir(1)–P(2)	2.330 (6)	Ir(1)–Cl(1)	2.562 (13)
Ir(1)–Cl(4)	2.50 (2)[a]	Ir(1)–C(1)	2.09 (2)
Ir(1)–C(3)	1.78 (2)		
		At Ir(2)	
Ir(1)–Ir(2)	2.887 (1)	Ir(2)–Ir(3)	2.842 (1)
Ir(2)–As(1)	2.404 (3)	Ir(2)–As(2)	2.422 (3)
Ir(2)–Cl(3)	2.57 (2)[a]	Ir(2)–C(1)	1.98 (2)
Ir(2)–C(2)	1.97 (3)		
		At Ir(3)	
Ir(3)–Ir(2)	2.842 (1)	Ir(3)–P(3)	2.342 (8)
Ir(3)–P(4)	2.362 (9)	Ir(3)–Cl(2)	2.599 (14)
Ir(3)–Cl(3)	2.47 (2)[a]	Ir(3)–C(2)	2.08 (3)
Ir(3)–C(4)	1.78 (3)		
		At Arsenic	
As(1)–C(18)	1.94 (3)	As(1)–C(17)	1.96 (3)
As(2)–C(49)	1.95 (2)	As(1)–C(24)	1.93 (3)
As(2)–C(56)	1.97 (3)	As(2)–C(50)	1.91 (3)
As(1)···P(1)	3.089 (7)	As(2)···P(2)	3.049 (7)
As(1)···P(3)	3.082 (7)	As(2)···P(4)	3.063 (7)
		At Phosphorus	
P(1)–C(11)	1.85 (2)	P(1)–C(5)	1.85 (3)
P(2)–C(37)	1.82 (2)	P(1)–C(17)	1.78 (2)
P(2)–C(49)	1.80 (2)	P(2)–C(43)	1.82 (3)
P(3)–C(25)	1.77 (3)	P(3)–C(24)	1.79 (3)
P(4)–C(56)	1.86 (2)	P(3)–C(31)	1.82 (3)
P(4)–C(63)	1.83 (2)	P(4)–C(57)	1.80 (3)
		Within Carbon Monoxide	
O(1)–C(1)	1.23 (3)	O(2)–C(2)	1.23 (4)
O(3)–C(3)	1.20 (3)	O(4)–C(4)	1.23 (3)

[a] Minor disordered form.

resonance at 184.0 ppm due to the bridging carbonyls. The triplet splitting on the terminal carbonyl resonance is due to coupling to the two cis phosphines (^2J(P,C) = 10.1 Hz). The corresponding splitting on the bridging resonance would be expected to be smaller and is not resolved. The ^{1}H NMR spectrum in the methylene region shows an AB quartet pattern with P–H coupling superimposed.

The X-ray diffraction data show a structure with unique environments for the two terminal iridium atoms and their ligands. In order to explain the NMR results, we postulate that in solution this cation undergoes the dynamic process involving bridge/terminal chloride exchange shown in eq 1. This process renders the

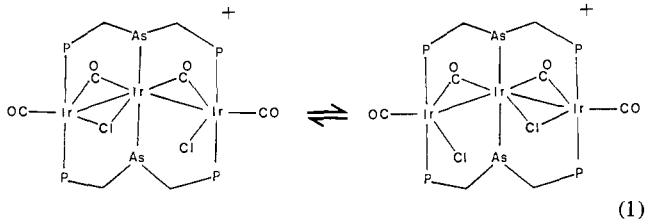

(1)

two phosphorus environments equivalent, makes the two methylene groups of dpma equivalent (while maintaining the intrinsic nonequivalence of the two protons within each methylene group), and interconverts the two bridging carbon monoxide ligands and the two terminal carbon monoxide ligands but does not interchange the bridge and terminal carbon monoxide environments. Analogous processes must also be occurring for the corresponding bromo and iodo complexes.

The trirhodium complexes also show spectroscopic features in solution which indicate that the two end phosphorus (and therefore rhodium) environments are equivalent. Relevant ^{31}P NMR spectra are shown in Figure 5. Trace A shows the spectrum of **4**. The pattern is similar to that of related compounds containing three unique phosphorus environments.[9,13] Trace B shows the spectrum of $[Rh_3(\mu\text{-dpmp})_2(\mu\text{-CO})_2(CO)_2(\mu\text{-I})I]^+$. Only two phosphorus environments, in a 2:1 intensity ratio, are detected. The corresponding spectrum for $[Rh_3(\mu\text{-dpmp})_2(\mu\text{-CO})_2(CO)_2(\mu\text{-Br})Br]^+$ shown in trace C is similar. The ^{31}P NMR spectrum of $[Rh_3(\mu\text{-dpma})_2(\mu\text{-CO})_2(CO)_2(\mu\text{-I})I]^+$ is even simpler since the central phosphorus and the spin–spin splitting it produces are removed. Consequently, the spectrum of this ion is a simple doublet (due to ^1J(Rh,P)) both at +25 and at −80 °C. The ^{1}H NMR spectra of these complexes show the presence of only two methylene environments, whereas similar dpmp-bridged complexes with inequivalent end PPh_2 groups must (and do)[13] produce four methylene resonances with H–H and H–P coupling superimposed.

Discussion

We take the structure of $[Ir_3(\mu\text{-dpma})_2(\mu\text{-CO})_2(CO)_2(\mu\text{-Cl})Cl]^+$ as determined by X-ray diffraction to be prototypical for the group of tetracarbonyls described here. Within this complex, each d^8 iridium(I) achieves an 18-electron count. In order to explain the multinuclear NMR results, we postulate the occurrence of the bridge/terminal chloride exchange shown in eq 1. This process requires a very minor movement of the atoms within the cation. Notice in Figures 2 and 4 that, except for the chloride ligands, the cation nearly has C_{2v} symmetry. In fact, the proposed motion described by eq 1 is closely related to the static disorder. To accomplish the movement required by eq 1, Cl(2) is required to move to a bridging site corresponding to that of Cl(3) and Cl(1) is required to move to a terminal site corresponding to that of Cl(4). The distances involved are only 1.54 (2) and 1.13 (2) Å, respectively. (It should be noted that these are not actual distances within any one cation in the solid.) A synchronous motion of this sort allows all iridium atoms to retain their 18-electron counts.

Unfortunately, the low-temperature limiting NMR spectra, which would display the asymmetry of the solid-state structure, are not found in the temperature range available to us. This leaves open the possibility of an alternate explanation: the presence of a different structure in solution. One structure that would accommodate these NMR results could be formed by breaking the Cl(1)–Ir(2) bond to give **7**. This would produce a coordinatively

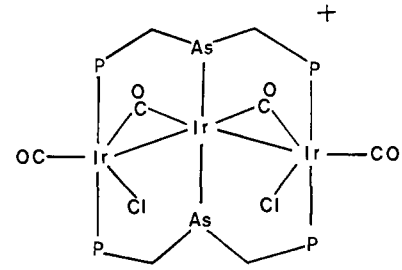

7

unsaturated, 16-electron center at the middle iridium, Ir(2), while leaving the terminal iridium centers coordinatively saturated and structurally equivalent. The process requires that movement of Cl(1) to the position of Cl(4) and breaking of the Cl(1)–Ir(2) bond occur upon dissolution. We disfavor this explanation because the similarity of the solution and solid-state infrared and electronic spectra of the complex indicates that similar structures are present in the solid and in solution.

Bridge/terminal chloride interchange has also been postulated for **2**. The process is described in eq 2. The required motion

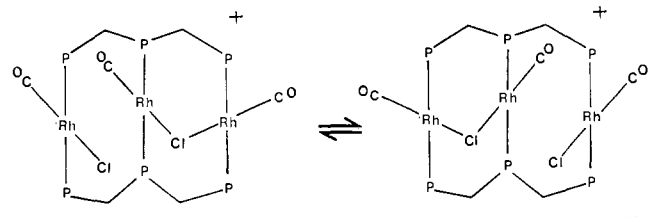

(2)

involves only ca. 1-Å displacements of the chloride ligands but a larger "wagging" of the central carbonyl groups. Again the dynamics are such that low-temperature limiting NMR spectra were not obtained. It is significant to note that while eq 1 involves

Table IV. Selected Interatomic Angles (deg) for $[Ir_3(\mu\text{-dpma})_2(\mu\text{-CO})_2(CO)_2(\mu\text{-Cl})Cl]^+$

			At Ir(1)				
Ir(2)–Ir(1)–P(1)	96.3 (1)	P(2)–Ir(1)–C(1)	99.2 (7)	Ir(2)–Ir(1)–P(2)	95.5 (1)	P(1)–Ir(1)–C(1)	98.5 (7)
P(1)–Ir(1)–P(2)	162.2 (2)	Cl(4)–Ir(1)–C(1)	129.9 (7)	Ir(2)–Ir(1)–Cl(1)	60.7 (3)	Cl(1)–Ir(1)–C(1)	104.1 (6)
P(1)–Ir(1)–Cl(1)	86.4 (4)	P(1)–Ir(1)–C(3)	89.5 (8)	P(2)–Ir(1)–Cl(1)	87.9 (3)	Ir(2)–Ir(1)–C(3)	146.0 (8)
Ir(2)–Ir(1)–Cl(4)	86.5 (3)[a]	Cl(1)–Ir(1)–C(3)	153.4 (8)	P(1)–Ir(1)–Cl(4)	84.3 (4)[a]	P(2)–Ir(1)–C(3)	88.1 (7)
P(2)–Ir(1)–Cl(4)	83.3 (4)[a]	C(1)–Ir(1)–C(3)	102.5 (10)	Cl(1)–Ir(1)–Cl(4)	25.8 (4)[a]	Cl(4)–Ir(1)–C(3)	127.6 (9)
Ir(2)–Ir(1)–C(1)	43.4 (6)						
			At Ir(2)				
Ir(1)–Ir(2)–As(1)	88.6 (1)	As(2)–Ir(2)–C(1)	90.0 (7)	Ir(3)–Ir(2)–As(1)	91.2 (1)	As(1)–Ir(2)–C(1)	91.7 (7)
Ir(1)–Ir(2)–As(2)	88.3 (1)	Ir(1)–Ir(2)–C(2)	147.0 (8)	Ir(3)–Ir(2)–As(2)	90.6 (1)	Cl(3)–Ir(2)–C(1)	158.2 (7)[a]
As(1)–Ir(2)–As(2)	173.8 (1)	As(1)–Ir(2)–C(2)	92.2 (9)	Ir(1)–Ir(2)–Cl(3)	112.0 (3)[a]	Ir(3)–Ir(2)–C(2)	47.0 (8)
Ir(3)–Ir(2)–Cl(3)	54.0 (3)[a]	Cl(3)–Ir(2)–C(2)	100.9 (9)[a]	As(1)–Ir(2)–Cl(3)	90.9 (4)[a]	As(2)–Ir(2)–C(2)	93.4 (9)
As(2)–Ir(2)–Cl(3)	85.3 (4)[a]	Ir(1)–Ir(2)–Ir(3)	166.0 (1)	Ir(1)–Ir(2)–C(1)	46.4 (7)	C(1)–Ir(2)–C(2)	100.6 (10)
Ir(3)–Ir(2)–C(1)	147.6 (7)						
			At Ir(3)				
Ir(2)–Ir(3)–P(3)	94.5 (2)	Ir(2)–Ir(3)–C(2)	43.9 (8)	C(2)–Ir(3)–C(4)	115.5 (13)	P(3)–Ir(3)–C(2)	97.1 (9)
P(3)–Ir(3)–P(4)	169.6 (2)	P(4)–Ir(3)–C(2)	92.9 (9)	Ir(2)–Ir(3)–P(4)	94.6 (2)	Cl(2)–Ir(3)–C(2)	136.5 (8)
P(3)–Ir(3)–Cl(2)	86.6 (4)	Cl(3)–Ir(3)–C(2)	101.3 (8)	Ir(2)–Ir(3)–Cl(2)	92.7 (2)	Ir(2)–Ir(3)–C(4)	159.3 (10)
Ir(2)–Ir(3)–Cl(3)	57.4 (3)[a]	P(3)–Ir(3)–C(4)	88.4 (10)	P(4)–Ir(3)–Cl(2)	88.1 (4)	P(4)–Ir(3)–C(4)	84.7 (10)
P(4)–Ir(3)–Cl(3)	91.2 (5)[a]	Cl(2)–Ir(3)–C(4)	107.9 (10)	P(3)–Ir(3)–Cl(3)	89.6 (4)[a]	Cl(3)–Ir(3)–C(4)	143.1 (11)[a]
			At Arsenic				
Ir(2)–As(1)–C(17)	111.6 (7)	Ir(2)–As(1)–C(18)	122.0 (10)	Ir(2)–As(2)–C(49)	110.0 (9)	Ir(2)–As(2)–C(50)	120.9 (7)
C(17)–As(1)–C(18)	104.9 (11)	Ir(2)–As(1)–C(24)	108.9 (10)	C(49)–As(2)–C(50)	105.8 (10)	Ir(2)–As(2)–C(56)	112.7 (8)
C(17)–As(1)–C(24)	101.8 (12)	C(18)–As(1–C(24)	105.6 (11)	C(49)–As(2)–C(56)	100.1 (10)	C(50)–As(2)–C(56)	105.2 (12)
			At Phosphorus				
Ir(1)–P(1)–C(5)	112.7 (8)	Ir(3)–P(3)–C(24)	111.6 (9)	Ir(1)–P(1)–C(11)	118.2 (10)	Ir(3)–P(3)–C(25)	112.9 (11)
C(5)–P(1)–C(11)	104.0 (12)	C(24)–P(3)–C(25)	106.2 (16)	Ir(1)–P(1)–C(17)	110.1 (9)	Ir(3)–P(3)–C(31)	117.1 (12)
C(5)–P(1)–C(17)	105.2 (12)	C(24)–P(3)–C(31)	103.4 (14)	C(11)–P(1)–C(17)	105.6 (10)	C(25)–P(3)–C(31)	104.7 (13)
Ir(1)–P(2)–C(37)	114.2 (9)	Ir(3)–P(4)–C(56)	110.9 (11)	Ir(1)–P(2)–C(43)	116.9 (7)	Ir(3)–P(4)–C(57)	116.0 (9)
C(37)–P(2)–C(43)	102.6 (10)	C(56)–P(4)–C(57)	106.1 (13)	Ir(1)–P(2)–C(49)	111.4 (8)	Ir(3)–P(4)–C(63)	116.4 (8)
C(37)–P(2)–C(49)	103.7 (11)	C(56)–P(4)–C(63)	99.7 (11)	C(43)–P(2)–C(49)	106.8 (13)	C(57)–P(4)–C(63)	106.2 (13)
			At Bridging Chloride				
Ir(1)–Cl(1)–Ir(2)	65.5 (5)	Ir(2)–Cl(3)–Ir(3)	68.6 (5)[a]				
			At Bridging Carbon Monoxide				
Ir(1–C(1)–Ir(2)	90.2 (10)	Ir(1)–C(1)–O(1)	132.5 (14)	Ir(3)–C(2)–O(2)	132.8 (18)	Ir(2)–C(2)–O(2)	137.9 (19)
Ir(2)–C(1)–O(1)	137.4 (16)	Ir(2)–C(2)–Ir(3)	89.1 (12)				
			At Terminal Carbon Monoxide				
Ir(1)–C(3)–O(3)	179.2 (21)	Ir(3)–C(4)–O(4)	168.6 (24)				
			At Methylene Carbons				
As(1)–C(24)–P(3)	111.9 (18)	As(1)–C(17)–P(1)	111.1 (14)	As(2)–C(56)–P(4)	106.1 (13)	As(2)–C(49)–P(2)	108.6 (13)

[a] Minor disordered form.

Table V. ^1H and ^{31}P NMR Data for Tetracarbonyl Complexes

	^{31}P		^1H				
	δ	^1J(Rh–P), Hz	δ_1	δ_2	J, Hz		
$[Rh_3(\mu\text{-dpmp})_2(\mu\text{-CO})_2(CO)_2(\mu\text{-Cl})Cl][BPh_4]$	27.1[a,b]	89					
	22.3[a,b]	105					
$[Rh_3(\mu\text{-dpmp})_2(\mu\text{-CO})_2(CO)_2(\mu\text{-Br})Br][BPh_4]$	25.6[a,b]	91					
	19.6[a,b]	105					
$[Rh_3(\mu\text{-dpmp})_2(\mu\text{-CO})_2(CO)_2(\mu\text{-I})I][BPh_4]$	21.4[b]	88					
	15.8[b]	106					
$[Rh_3(\mu\text{-dpma})_2(\mu\text{-CO})_2(CO)_2(\mu\text{-I})I][BPh_4]$	23.5[b]	92	4.05	4.73	12.0 (H,H)	2.9 (H,P)	4.5 (H,P)
	23.5[a,b]	91					
$[Ir_3(\mu\text{-dpma})_2(\mu\text{-CO})_2(CO)_2(\mu\text{-Cl})Cl][BPh_4]$	−0.75		3.76	4.16	12.5 (H,H)	2.9 (H,P)	4.7 (H,P)
	−1.5[a]						
$[Ir_3(\mu\text{-dpma})_2(\mu\text{-CO})_2(CO)_2(\mu\text{-Br})Br][BPh_4]$	−4.6		4.04	4.31	12.5 (H,H)	2.9 (H,P)	2.9 (H,P)
	−5.2[a]						
$[Ir_3(\mu\text{-dmpa})_2(\mu\text{-CO})_2(CO)_2(\mu\text{-I})I][BPh_4]$	−11.1		4.49	4.60	12.3 (H,H)	2.8 (H,P)	4.2 (H,P)
	−11.4[a]						

[a] At −75 °C. [b] Recorded in the presence of CO gas.

a coordinatively saturated complex, eq 2 involves an unsaturated species in which each metal is a 16-electron center.

The spectroscopic data indicate that all of the rhodium and iridium complexes of the tetracarbonyl family considered here have similar structures. Thus, unlike the tricarbonyl family, the structure is not changed when the halide is changed. Also, the tetracarbonyl family shows rapid bridge/terminal interchange for each of the three halides examined. The similarity of rhodium and iridium structures is exactly what one would expect given their isolobal and isoelectronic character and their similar sizes.

Experimental Section

Preparation of Compounds. The ligands dpmp[1] and dpma[2] were prepared as described previously as were the complexes **2**,[9] **3**,[13] **4**,[13] and $Ir(CO)_2Cl(p\text{-tld})$.[14] The syntheses of the iridium compounds were carried out under a purified dinitrogen atmosphere.

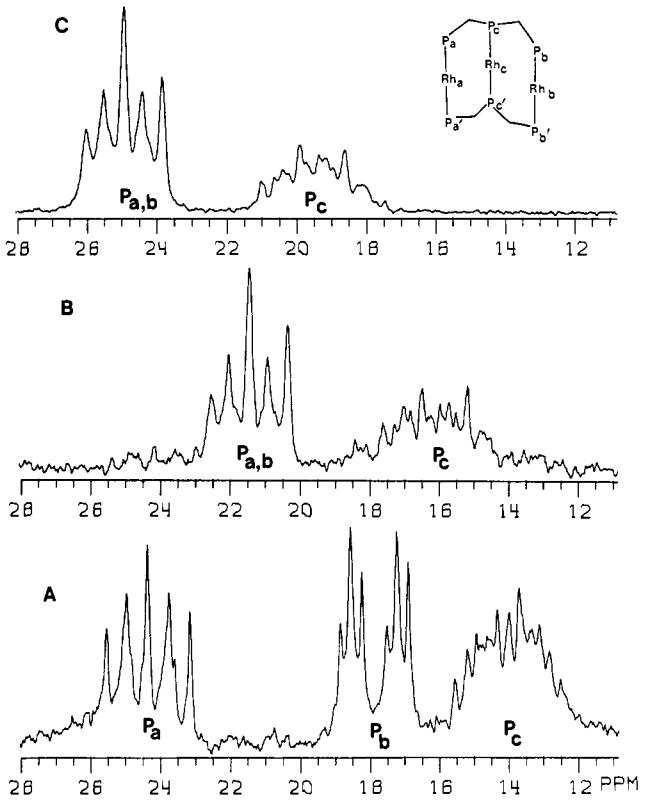

Figure 5. ^{31}P NMR spectra of dichloromethane solutions of (A) $[Rh_3(\mu\text{-dpmp})_2(\mu\text{-CO})(CO)_2(\mu\text{-I})_2]^+$ at 25 °C, (B) $[Rh_3(\mu\text{-dpmp})_2(\mu\text{-CO})_2(CO)_2(\mu\text{-I})I]^+$ at 25 °C, and (C) $[Rh_3(\mu\text{-dpmp})_2(\mu\text{-CO})_2(CO)_2(\mu\text{-Br})Br]^+$ at −80 °C.

$[Ir_3(\mu\text{-dpma})_2(\mu\text{-CO})_2(CO)_2(\mu\text{-Cl})Cl][BPh_4]$. A solution of 106 mg (0.271 mmol) of $Ir(CO)_2Cl(p\text{-tld})$ in 4 mL of dichloromethane was added slowly (10 min) with stirring to a solution of 100 mg (0.182 mmol) of dpma and 50 mg (0.15 mmol) of sodium tetraphenylborate in 4 mL of dichloromethane and 2 mL of methanol. After the mixture was stirred for an additional 2 h, 10 mL of methanol was added slowly to precipitate the orange crystalline product. The product was collected by filtration and washed successively with methanol and diethyl ether. The product was purified by dissolving it in a minimum amount of dichloromethane, filtering, and slowly adding diethyl ether. The crystalline product was collected by filtration and washed with diethyl ether; yield 0.075 g, 38%. Anal. Calcd for $C_{92}H_{78}As_2BCl_2Ir_3O_4P_4$: C, 50.70; H, 3.61; Cl, 3.25. Found: C, 50.79; H, 3.51; Cl, 3.50.

$[Rh_3(\mu\text{-dpma})_2(\mu\text{-CO})_2(CO)_2(\mu\text{-I})I][BPh_4]$. Carbon monoxide was bubbled through a filtered solution of 100 mg (0.048 mmol) of $[Rh_3(\mu\text{-dpma})_2(\mu\text{-CO})(CO)_2(\mu\text{-I})_2][BPh_4]$[4] dissolved in a minimum quantity of dichloromethane. The initially brown solution rapidly became red, and after several minutes crystals began to precipitate. After 1 h the flow of carbon monoxide was stopped and the black, crystalline product collected by filtration and washed with diethyl ether; yield 0.095 g, 95%. Anal. Calcd for $C_{92}H_{78}As_2BI_2O_4P_4Rh_3$: C, 52.75; H, 3.75; I, 12.12. Found: C, 52.72; H, 3.73; I, 12.3.

$[Rh_3(\mu\text{-dpmp})_2(\mu\text{-CO})_2(CO)_2(\mu\text{-I})I][BPh_4]$. The above procedure for the preparation of $[Rh_3(\mu\text{-dpma})_2(\mu\text{-CO})_2(CO)_2(\mu\text{-I})I][BPh_4]$ was employed, with 100 mg (0.05 mmol) of $[Rh_3(\mu\text{-dpmp})_2(\mu\text{-CO})(CO)_2(\mu\text{-I})_2][BPh_4]$ (**4**) as the starting material; yield 0.090 g, 90%. Because of the ready loss of carbon monoxide from the solid and the likelihood of the presence of lattice-trapped dichloromethane, the solid was not subjected to elemental analysis.

$[Rh_3(\mu\text{-dpmp})_2(\mu\text{-CO})_2(CO)_2(\mu\text{-Br})Br][BPh_4]$. The above procedure for the preparation of $[Rh_3(\mu\text{-dpmp})_2(\mu\text{-CO})_2(CO)_2(\mu\text{-I})I][BPh_4]$ was employed, with 80 mg (0.04 mmol) of $[Rh_3(\mu\text{-dpmp})_2(\mu\text{-CO})(CO)_2Br_2][BPh_4]$ as the starting material. The solution volume was reduced by approximately half under a carbon monoxide purge in order to induce precipitation of the red, crystalline product; yield 0.060 g, 75%. Because of the ready loss of carbon monoxide from the solid and the likelihood of the presence of lattice-trapped dichloromethane, the solid was not subjected to elemental analysis.

$[Ir_3(\mu\text{-dpma})_2(\mu\text{-CO})_2(CO)_2(\mu\text{-I})I][BPh_4]$. A solution of 150 mg (0.44 mmol) of sodium tetraphenylborate in 1 mL of methanol was added to a solution of 90 mg (0.041 mmol) of $[Ir_3(\mu\text{-dpma})_2(\mu\text{-CO})_2(CO)_2(\mu\text{-Cl})Cl][BPh_4]$ in 10 mL of dichloromethane. The light green-orange solution immediately turned deep green. A solution of 35 mg (0.23 mmol) of sodium iodide in 1 mL of methanol was then added to the reaction mixture, and the color immediately turned orange. Bright orange crystals began to precipitate after several minutes. Five milliliters of methanol was added slowly, and the solution was allowed to stand for 1 h. The orange, crystalline product was collected by filtration and washed with methanol and diethyl ether; yield 0.065 g, 67%. Anal. Calcd for $C_{92}H_{78}As_2BI_2Ir_3O_4P_4$: C, 46.77; H, 3.33; I, 10.74. Found: C, 46.31; H, 3.18; I, 10.94.

$[Ir_3(\mu\text{-dpma})_2(\mu\text{-CO})_2(CO)_2(\mu\text{-Br})Br][BPh_4]$. The procedure for the preparation of $[Ir_3(\mu\text{-dpma})_2(\mu\text{-CO})_2(CO)_2(\mu\text{-I})I][BPh_4]$ was employed, the sodium iodide solution being replaced with one of 35 mg (0.34 mmol) of sodium bromide in 5 mL of methanol. Light orange crystals precipitated several minutes after the addition of sodium bromide, and these were collected by filtration and washed with methanol and diethyl ether; yield 0.060 g, 64%. Anal. Calcd for $C_{92}H_{78}As_2BBr_2Ir_3O_4P_4$: C, 48.71; H, 3.47; Br, 7.04. Found: C, 48.27; H, 3.30; Br, 7.27.

Table VI. Crystal Data for $[Ir_3(\mu\text{-dpma})_2(\mu\text{-CO})_2(CO)_2(\mu\text{-Cl})Cl][B(C_6H_5)_4]\cdot 2CH_2Cl_2$

formula	$C_{96}H_{106}As_2BCl_{10}Ir_3O_4P_4$
fw (incl solvent)	2536
cryst syst	triclinic
space group	$P\bar{1}$ (No. 2)
cryst dimens, mm	0.25 × 0.30 × 0.37
color and habit	yellow-brown parallelepipeds
unit cell dimens (140 K)	
a, Å	12.789 (3)
b, Å	16.936 (4)
c, Å	23.874 (6)
α, deg	87.80 (2)
β, deg	68.69 (2)
γ, deg	77.05 (2)
V, Å^3	4690 (2)
ρ(calcd), g cm^{-3} (at 140 K)	1.680[a]
Z	2
radiatn, λ, Å (graphite monochromator)	Mo K$\bar{\alpha}$, 0.71069
μ(Mo Kα), cm^{-1}	56.6
range of abs cor factors	3.22–6.00
scan type ($2\theta_{max}$, deg)	ω (45)
scan range, deg	1.2
octants	$+h,\pm k,\pm l$
scan speed, deg min^{-1}	60
check reflecns, interval no.	2 mesd every 200 reflecns
no. of unique data	12225
no. of data $I > 3\sigma(I)$	8413
R	0.083
R_w	0.090
no. of params	493

[a] Calculated for 2 CH_2Cl_2, the approximate content of dichloromethane obtained from refinement.

Spectroscopic Measurements. The ^{31}P NMR spectra were recorded with proton decoupling on a Nicolet NT 200 Fourier transform spectrometer operating at 81 MHz or on a Nicolet NT-360 spectrometer at 145.8 MHz. The ^1H and ^{13}C NMR spectra were recorded at 360 and 90.5 MHz, respectively, on a Nicolet NT-360 FT spectrometer. The references were as follows: ^{31}P, external 85% phosphoric acid; ^1H, ^{13}C, internal tetramethylsilane. The high-frequency-positive convention, recommended by IUPAC, has been used in reporting all chemical shifts. Infrared spectra were recorded from mineral oil mulls or dichloromethane solutions with a Perkin-Elmer 180 spectrometer. Electronic spectra were recorded on a Hewlett-Packard 8450A or a Cary 17 spectrophotometer.

X-ray Data Collection, Solution, and Refinement for $[Ir_3(\mu\text{-dpma})_2(\mu\text{-CO})_2(CO)_2(\mu\text{-Cl})Cl][B(C_6H_5)_4]\cdot 2CH_2Cl_2$. Well-formed yellow-brown parallelepipeds were grown by slow diffusion of diethyl ether through a 3-mm layer of methanol into a dichloromethane solution of the complex. Crystal data, data collection procedures, and refinement of the structure are summarized in Table VI. The lattice was found to be triclinic by standard procedures using the software associated with the Syntex $P2_1$ diffractometer. The data were collected at 140 K with use of a locally modified LT-1 low-temperature apparatus on the Syntex $P2_1$ diffractometer. The data were corrected for Lorentz and polarization effects.

The structure was solved by locating the iridium atoms with use of the Patterson method (FMAP 8 routine of SHELXTL, version 4, 1984 (Nicolet Instrument Corp., Madison, WI)). Other atoms were located from successive difference Fourier maps. During refinement it became apparent that the chloride ligands in the cation were disordered. Two sets

of alternate positions, one involving Cl(1) and Cl(2) and the other involving Cl(3) and Cl(4), were allowed to refine with an occupancy of k assigned to the first set and $1 - k$ assigned to the second set. The chloride ligands were given equivalent isotropic U values of 0.04 Å^2. Refinement yielded $k = 0.548$ (7). Since the disorder in atoms Cl(1), Cl(2), Cl(3), and Cl(4) corresponded to approximately 50% occupancy for these atoms, the possibility that the noncentrosymmetric space group $P1$ could resolve this disorder was investigated. However, a difference map computed in $P1$ clearly revealed the presence of all four chlorines in both of the triiridium complexes. Thus, we conclude that the disorder results from a distribution of the two forms of the molecule in a lattice site that does not discriminate between these two forms. Final cycles of refinement were made with anisotropic thermal parameters for iridium, arsenic, and phosphorus and isotropic thermal parameters for all remaining atoms. Hydrogen atoms were refined with use of a riding model in which an idealized C–H vector of 0.96-Å length is recalculated with each cycle of refinement. Isotropic hydrogen thermal parameters were fixed at 1.2 times the equivalent isotropic thermal parameter of the bonded carbon. Scattering factors and corrections for anomalous dispersion were taken from a standard source.[22] An absorption correction (XABS) was applied.[23] The atoms of four dichloromethane molecules were assigned equivalent isotropic U values of 0.07 Å^2 and were allowed to refine with variable occupancy. The final occupancies were 0.643 (12) for Cl(5)···Cl(6), 0.654 (12) for Cl(7)···Cl(8), 0.425 (13) for Cl(9)···Cl(10), and 0.373 (12) for Cl(11)···Cl(12). Carbon atoms for the last two dichloromethanes were not located due to the low occupancy and disorder. Two low-angle reflections suffering from extinction were removed from the data set for the final cycles of refinement. A conventional R factor of 0.083 was obtained. The final difference map showed some residual electron density in the vicinity of the dichloromethane molecules, but otherwise no significant features were present.

Acknowledgment. We thank the National Science Foundation (Grant No. CHE8217954) for financial support and Dow Corning Corp. for a fellowship for P.E.R.

Registry No. **2**, 84774-74-3; **3**, 100700-65-0; **4**, 86372-61-4; $[Rh_3(\mu\text{-dpmp})_2(\mu\text{-CO})_2(CO)_2(\mu\text{-Cl})Cl][BPh_4]$, 100700-67-2; $[Rh_3(\mu\text{-dpmp})_2(\mu\text{-CO})_2(CO)_2(\mu\text{-Br})Br][BPh_4]$, 100700-69-4; $[Rh_3(\mu\text{-dpmp})_2(\mu\text{-CO})_2(CO)_2(\mu\text{-I})I][BPh_4]$, 100700-71-8; $[Rh_3(\mu\text{-dpma})_2(\mu\text{-CO})_2(CO)_2(\mu\text{-I})I][BPh_4]$, 100700-73-0; $[Ir_3(\mu\text{-dpma})_2(\mu\text{-CO})_2(CO)_2(\mu\text{-Cl})Cl][BPh_4]$, 100700-76-3; $[Ir_3(\mu\text{-dpma})_2(\mu\text{-CO})_2(CO)_2(\mu\text{-Br})Br][BPh_4]$, 100700-78-5; $[Ir_3(\mu\text{-dpma})_2(\mu\text{-CO})_2(CO)_2(\mu\text{-I})I][BPh_4]$, 100700-80-9; $Ir(CO)_2Cl(p\text{-tld})$, 14243-22-2; $[Rh_3(\mu\text{-dpma})_2(\mu\text{-CO})(CO)_2(\mu\text{-I})_2][BPh_4]$, 100700-82-1.

Supplementary Material Available: Listings of hydrogen atom positions, bond lengths, bond angles, anisotropic thermal parameters, and structure factor amplitudes (55 pages). Ordering information is given on any current masthead page.

(22) "International Tables for X-ray Crystallography"; Kynoch Press: Birmingham, England, 1974; Vol. 4.
(23) The method obtains an empirical absorption tensor from an expression relating F_o and F_c: Hope, H.; Moezzi, B. Department of Chemistry, University of California: Davis, CA.

Contribution from the Laboratoire de Physicochimie Minérale, CNRS, UA 420, and LURE,[1] Université Paris Sud, 91405 Orsay, France

Coordination Chemistry of the Lamellar MPS_3 Materials: Metal–Ligand Cleavage as the Source of an Unusual "Cation-Transfer" Intercalation Process

Renê Clement,* Odile Garnier, and Jocelyne Jegoudez

Received August 8, 1985

Several MPS_3 lamellar materials exhibit a very unusual intercalation chemistry based on a "cation-transfer" process between the solid and a solvent. This contrasts with the electron-transfer process that governs the intercalation chemistry of the layered dichalcogenides MX_2. Although the MPS_3 layers are made up of infinite arrays of $P_2S_6^{4-}$ units coordinated to the M^{2+} cations, the metal–ligand (M–S) bonding still exhibits enough lability to allow the M^{2+} cations to jump, under very mild conditions, from intra- toward interlamellar sites (or the opposite) and even to be removed from the material, provided a suitable cation is available to intercalate the lattice and maintain electrical neutrality. Depending on the metal, the solvent, and the guest species, the reaction may take place spontaneously or require an assist, usually by complexing the leaving M^{2+} cations (EDTA). Small inserted ions (Na^+, K^+, ...) are strongly solvated and mobile, and they can in turn be exchanged. To rationalize this behavior, we suggest that the intercalation chemistry of the MPS_3 involves a chemical transformation of the whole of the material, rather than a diffusional process of the guest species within the host lattice. The MPS_3 layered materials are considered as polynuclear complexes that can undergo heterogeneous equilibrium with their constitutive species M^{2+} and $P_2S_6^{4-}$ and other species present in solution. In support of this mechanism, MPS_3 materials have been successfully prepared by mixing aqueous solutions of $Na_4P_2S_6$ and transition-metal salts. Some implications of this mechanism are discussed.

I. Introduction

Transition-metal hexathiohypodiphosphates MPS_3, where M stands for a metal in the II oxidation state, form a class of lamellar semiconductors first described by Klingen.[2] The structure of these materials (Figure 1) is closely related to that of the well-known transition-metal dichalcogenides MX_2 and for this reason, the MPS_3 compounds have been merely considered in the beginning as an exotic appendix of this wide class. Indeed, the early chemistry carried out in the series supported this analogy: as well as the MX_2 compounds, several MPS_3 compounds have been shown to react with electron-donor species (butyllithium, cobaltocene) to form intercalation compounds and to behave as good cathode materials in secondary lithium batteries.[3-5]

A few years ago, one of us discovered that $MnPS_3$ could spontaneously react at room temperature with aqueous solutions of certain salts, such as KCl and NH_4Cl and salts of small organometallic cations such as cobaltocenium;[6] this reaction led to compounds of the type $Mn_{1-x}PS_3[G]_{2x}(H_2O)_y$, where the positive charge of the guest cation G^+ was counterbalanced by the removal of an equivalent amount of intralayer Mn^{2+} cations. The host structure was observed to remain solid throughout the reaction process, and therefore such an exchange process appeared rather unusual, as no similar reaction had been described in any other layered system. Furthermore, small inserted cations such as K^+ or NH_4^+ were found to be strongly solvated and highly mobile,

* To whom correspondence should be addressed at the Laboratoire de Physicochimie Minérale.

(1) LURE: CNRS laboratory for synchrotron radiation, associated with the Université de Paris Sud.
(2) (a) Klingen, W.; Ott, R.; Hahn, H. *Z. Anorg. Allg. Chem.* **1973**, *396*, 271. (b) Klingen, W.; Eulenberger, G.; Hahn, H. *Ibid.* **1973**, *401*, 97.
(3) Clement, R.; Green, M. L. H. *J. Chem. Soc., Dalton Trans.* **1979**, 1566.
(4) Brec, R.; Schleich, D. M.; Ouvrard, G.; Louisy, A.; Rouxel, J. *Inorg. Chem.* **1979**, *18*, 1814.
(5) Johnson, J. W. In *Intercalation Chemistry*; Whittingham, M. S., Jacobson, A. J., Eds.; Academic: New York, 1982.
(6) Clement, R. *J. Chem. Soc., Chem. Commun.* **1980**, 647.

0020-1669/86/1325-1404$01.50/0